ORGANIC CHEMISTRY

FRONTIERS

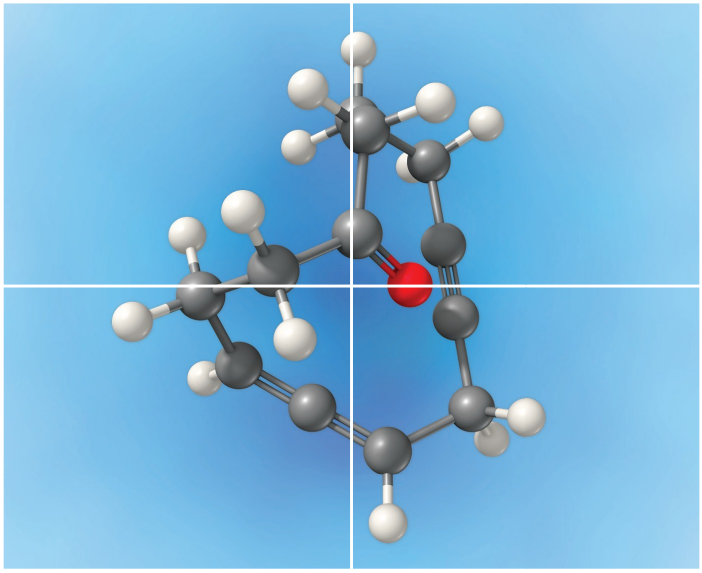

Accepted Manuscript

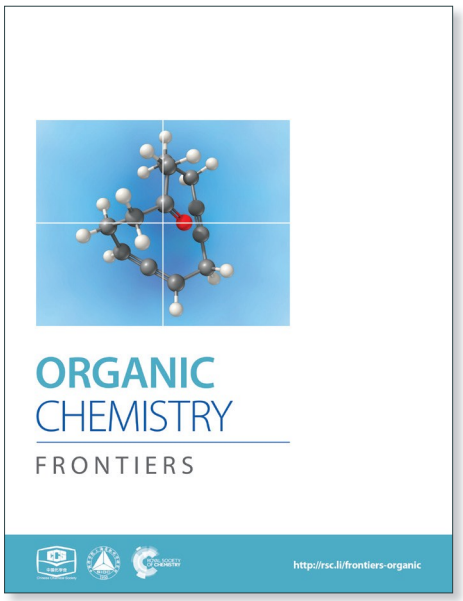

This is an *Accepted Manuscript*, which has been through the Royal Society of Chemistry peer review process and has been accepted for publication.

Accepted Manuscripts are published online shortly after acceptance, before technical editing, formatting and proof reading. Using this free service, authors can make their results available to the community, in citable form, before we publish the edited article. We will replace this *Accepted Manuscript* with the edited and formatted *Advance Article* as soon as it is available.

You can find more information about *Accepted Manuscripts* in the **Information for Authors**.

Please note that technical editing may introduce minor changes to the text and/or graphics, which may alter content. The journal's standard **Terms & Conditions** and the **Ethical guidelines** still apply. In no event shall the Royal Society of Chemistry be held responsible for any errors or omissions in this *Accepted Manuscript* or any consequences arising from the use of any information it contains.

Quantum mechanical study of mechanism and stereoselectivity on the N-heterocyclic carbene catalyzed [4 + 2] annulation reaction of enals with azodicarboxylates

Yang Wang, Linjie Zheng, Donghui Wei[1], and Mingsheng Tang[2]
The College of Chemistry and Molecular Engineering, Center of Computational Chemistry, Zhengzhou University, Zhengzhou, Henan Province, 450001, P.R. China

Abstract

A systematic theoretical study has been carried out to understand the mechanism and stereoselectivity of [4 + 2] annulation reaction between γ-oxidized enals and azodicarboxylates catalyzed by the N-heterocyclic carbene (NHC). The calculated results reveal that the catalytic cycle can be characterized by three stages (**Stage**s **1**, **2**, and **3**). **Stage 1** is the nucleophilic addition of NHC catalyst to enals upon the intramolecular proton transfer to generate the Breslow intermediate. In this stage, except the direct proton transfer mechanism, the H_2O (H_2O and $2H_2O$ cluster) and bicarbonate anion (HCO_3^-) mediated proton transfer mechanism are also investigated, the free energy barrier for the crucial proton transfer steps in **Stage 1** is found to be significantly lower by explicit inclusion of bicarbonate anion (HCO_3^-). For **Stage 2**, the removal of the leaving group occurs, followed by C–C bond rotation for the formation of *cis*-dienolate. **Stage 3** is the *endo*/*exo* [4 + 2] cycloaddition and dissociation of catalyst from the final products. The formal [4 + 2] cycloaddition step is calculated to be the enantioselectivity determining step, and the R-configured **PR** is the predominated product according to the computations, which is in good agreement with the experimental observations. Moreover, the stereoselectivity associated with the chiral carbon center is attributed to the CH-π interaction between C^{α}–H and mesityl group of NHC and the variation in the distortion of the dienolate. The mechanistic insights obtained in the present study should be valuable for the other NHC-catalyzed reactions.

Keywords: N-heterocyclic carbene, [4 + 2] annulation, Density functional theory

[1] Corresponding author: donghuiwei@zzu.edu.cn (D.-H. Wei)
[2] Corresponding author: mstang@zzu.edu.cn (M.-S. Tang)

1. Introduction

N-heterocyclic carbene (NHC) has been widely applied in the form of ligands,[1] and Lewis base catalysts.[2] As an important organocatalyst, NHC have been successfully used in carbon-carbon and carbon-heteroatom bond formation reactions including cross-benzoin, Stetter, homoenolate, annulation, and cycloaddition reactions.[3] In the past few years, Lewis base NHC has been found to be the powerful organocatalyst in the stereoselective cycloaddition reactions of ketene, including the [2 + 2],[4] [2 + 2 + 2],[4d,5] and [4 + 2][6] cycloaddition reactions. While for the annulation reactions catalyzed by NHC, the enals are frequently used as one of the reactants. Due to the special reactivity of the reactants (i.e. ketene and enals), their NHC-catalyzed cycloaddition/annulation reactions can provide a facile and also effective access to a variety of ring skeletons, especially for construction N/O-containing heterocycles.

In the NHC catalyzed annulation reaction, the enals can react with a variety of electrophilic coupling partners, such as alkenes, imines, and ketones. The addition of NHC catalyst to the enals can lead to different reactive intermediates bearing more than one reactive carbon centers of the enals, such as the homoenolate intermediate (β-carbon),[7] enolate intermediate (α-carbon),[8] and acyl anion equivalent intermediate (carbonyl carbon),[9] which allows the inversion of the normal reactivity (umpolung) through formation of Breslow intermediates and serve as the prenucleophiles. In these reactions, the enals can function as two-, three-, and four-carbon synthons under going [2 + 4],[8e,10] [3 + n] (n=2, 3, 4),[3k,11] and [4 + n] (n=2, 3)[12] annulation reactions. In 2004, Glorius group[7a] and Bode group[7b] concurrently reported the NHC-catalyzed annulation reaction of enals with aldehydes to afford the γ-lactones, in which the enal β-carbon severed as the reactive nucleophilic carbon. Then, the same kind of reaction had been further extensively explored by many other groups. The reactivity of the enal α-carbon reaction has also been well studied by Bode,[8a] Glorius,[8b] Scheidt,[8c] Nair,[8d] and Chi.[8e]

In contrast to the α- and β-carbons of enal, the activated γ-carbon of enal worked as the four-carbon synthon is much less studied in the past years. There are only few successful examples in NHC-mediated γ-functionalization of the enals by activating the enal γ-carbon as nucleophiles.[13] In 2012, Chi and coworkers reported the pioneering work of the oxidative NHC-catalyzed [4 + 2] annulation of enals with trifluoromethyl ketones by γ addition,[13a] then they reported the first NHC-catalyzed [3

+ 4] annulation reaction[13d] of enals with azomethine imines by activating the γ-carbon of enals as 1,4-dipolarophile. Ye et al. reported the NHC-catalyzed [4 + 2] annulation of γ-oxidized enals with azodicarboxylates in good yield and with excellent enantioselectivity.[13b]

With the development of NHC-catalyzed annulation reactions of enals in experiment, the theoretical investigations on the mechanisms have also been reported in literature.[14] For example, Bode and coworkers computationally studied the NHC-catalyzed [4 + 2] cycloaddition reaction of α,β-unsaturated aldehyde (C2-synthon) with enone, they identified that the oxyanion-steering mechanism and CH-π interaction are the two crucial interactions for the high selectivity.[14c] Sunoj et al. performed a theoretical investigation on the mechanism and stereoselectivity in a chiral N-heterocyclic carbene-catalyzed cycloannulation reaction of the homoenolate derived from butenal with pentenone.[14d] More recently, we have performed the theoretical investigation on the mechanism of the NHC-catalyzed [4 + 2] annulation reaction of enals (C2-synthon) and chalcones, and the computational results show that the acetic acid can assist the proton transfer process.[14e] To the best of our knowledge, the computational investigation on the mechanism and enantioselectivity of NHC-catalyzed [4 + 2] annulation of enals (C4-synthon) by γ addition has remained hitherto unexplored.

It is noteworthy that the mechanisms and stereoselectivities of NHC-catalyzed [2 + 2],[15] [4 + 2],[16] [2 + 2 + 2][17] cycloaddition reactions of ketene have been studied by our group using DFT methods. Actually, the reaction mechanism might be diverse for different NHC catalytic cycloadditions of ketene, these cycloaddition reactions do not always initiate by the reaction of NHC with ketene.[16] As known to all, there exists the proton transfer process involved in the NHC-catalyzed annulation reaction of enals, which is remarkably different from the cycloaddition reaction, and this would make the reaction mechanism more complicated. Correspondingly, the mechanism of NHC-catalyzed annulation reactions of enals should be also multiple, which is because the catalysts, reactants, and additives will influence the proton transfer process involved in this kind of reactions. Thus, the theoretical investigation is necessary for these special organocatalytic reactions.

In this present study, we aim to disclose the mechanism and enantioselectivity of NHC-catalyzed [4 + 2] annulation reaction of γ-oxidized enals and azodicarboxylates reported by Ye and co-workers (**Scheme 1**).[13b] On the basis of the presumptive

mechanism proposed by Ye, we suggested the possible mechanism on the reaction of enals with azodicarboxylates catalyzed by NHC (shown in **Scheme 2**): Initially, NHC nucleophilic attacks on the enal for the formation of zwitterionic intermediate **I**. Subsequently, the intermediate **I** transforms to the Breslow intermediate **II** via the proton transfer process. Then the removal of the leaving group (LG) generates the *trans*-dienolate **III** by abstracting the hydride from the carbonyl oxygen, which affords vinyl enolates as the reactive 1,4-dipolarophile. The fourth step is the [4 + 2] cycloaddition of **III** with azodicarboxylates for the formation of the adduct **IV**, and finally the dissociation of the desired products **PR&PS** and regeneration of catalyst **Cat**.

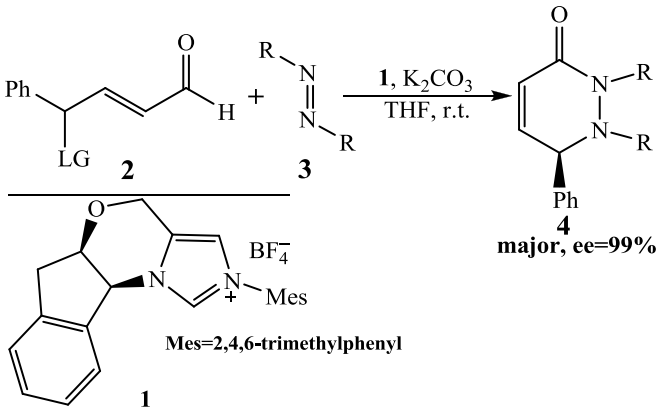

Scheme 1 The NHC-catalyzed [4 + 2] annulation reaction of enals with azodicarboxylates

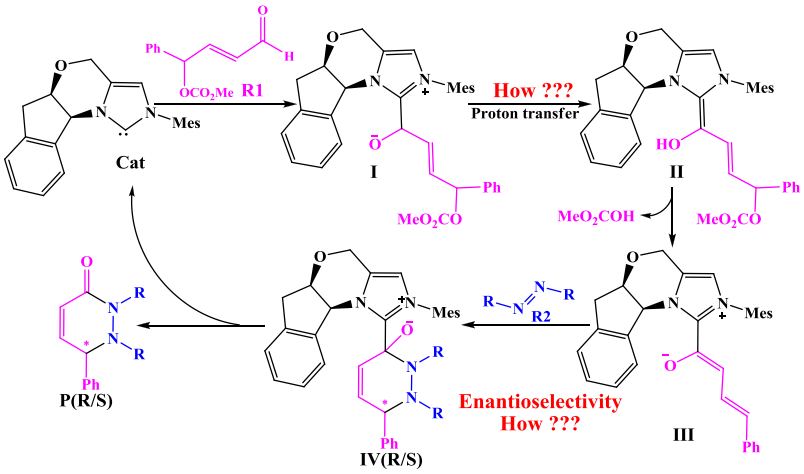

Scheme 2 The proposed catalytic cycle of the [4 + 2] annulation reaction

Nevertheless, there are still some issues need to be settled as shown in **Scheme 2**: In the second step, the direct 1,2-proton transfer process would cost quite high energy

barrier due to the large strain in the three-membered ring transition state. Moreover, the reaction proceeds without protic additive in the reaction system, thus how does the 1,2-proton transfer happen? As the design of new organocatalyst relies on a detailed understanding of the underlying factors that governing the enantioselectivity of this kind of reactions, thus what is the main factors that controlling the enantioselectivity of this reaction? With these questions as motivation, the present work will pursue a theoretical investigation on the title reaction to not only obtain a preliminary picture from the γ-oxidized enal [4 + 2] annulation reaction, but also explore the factors that controlling the stereochemistry of this reaction. And we believe that the mechanistic information should be important for understanding the NHC-catalyzed [4 + 2] annulation reactions and providing novel insights into recognizing this kind of reaction in detail.

For sake of convenience, the [4 + 2] annulation reaction between the γ-oxidized enals (**R1**, LG=OCO_2Me, **Scheme 2**) and di-*tert*-butyl azodicatboxylate (**R2**, **Scheme 2**) catalyzed by NHC (**Cat**, **Scheme 2**) have been chosen as the objects of investigation. In the present study, we will give the computational results for the possible reaction mechanisms to illustrate the theoretical methodology for this issue at the molecular level using the density functional theory (DFT), which has been widely used in the study of organic,[18] biological reaction mechanisms,[19] and others.[20]

2. Computational Details

Quantum mechanical calculations reported herein were carried out by using density functional theory with the *Gaussian 09* suite of programs.[21] The solution-phase geometry optimization of all species is performed with the recently developed M06-2X[22] density functional along with the 6-31G(d, p) basis set in THF solvent using the integral equation formalism polarizable continuum model (IEF-PCM).[23] The harmonic vibrational frequency calculations were performed at the same level of theory as that used for geometry optimizations to provide thermal corrections of Gibbs free energies and make sure that the local minima had no imaginary frequencies, while the saddle points had only one imaginary frequency. Intrinsic reaction coordinates (IRCs)[24] were calculated to confirm that the transition state structure connected the correct reactant and product on the potential energy surface, and the natural bond orbital (NBO)[25] analysis was employed to assign the

atomic charges. The three dimensional structures had been represented in the figures by using the CYLView software.[26]

We choose to discuss this theoretical study based on the solution-phase Gibbs free energies calculated by the M06-2X/6-31G(d, p)/IEF-PCM$_{(THF)}$ method rather than Born-Oppenheimer energies, which are the electronic (including nuclear-repulsion) energies plus zero-point vibrational energies (ZPVEs).

3. Results and Discussions

As shown in **Schemes 3** and **4**, the suggested mechanism for each elementary step of the annulation reaction between **R1** and **R2** catalyzed by **Cat** includes three stages, i.e. the formation of Breslow intermediate (**Stage 1, Scheme 3**), formation of the *cis*-dienolate (**Stage 2**, **Scheme 4**), and formal [4 + 2] cycloaddition and regeneration of catalyst (**Stage 3**, **Scheme 4**). In the following parts of this section, we will give detailed discussions step by step.

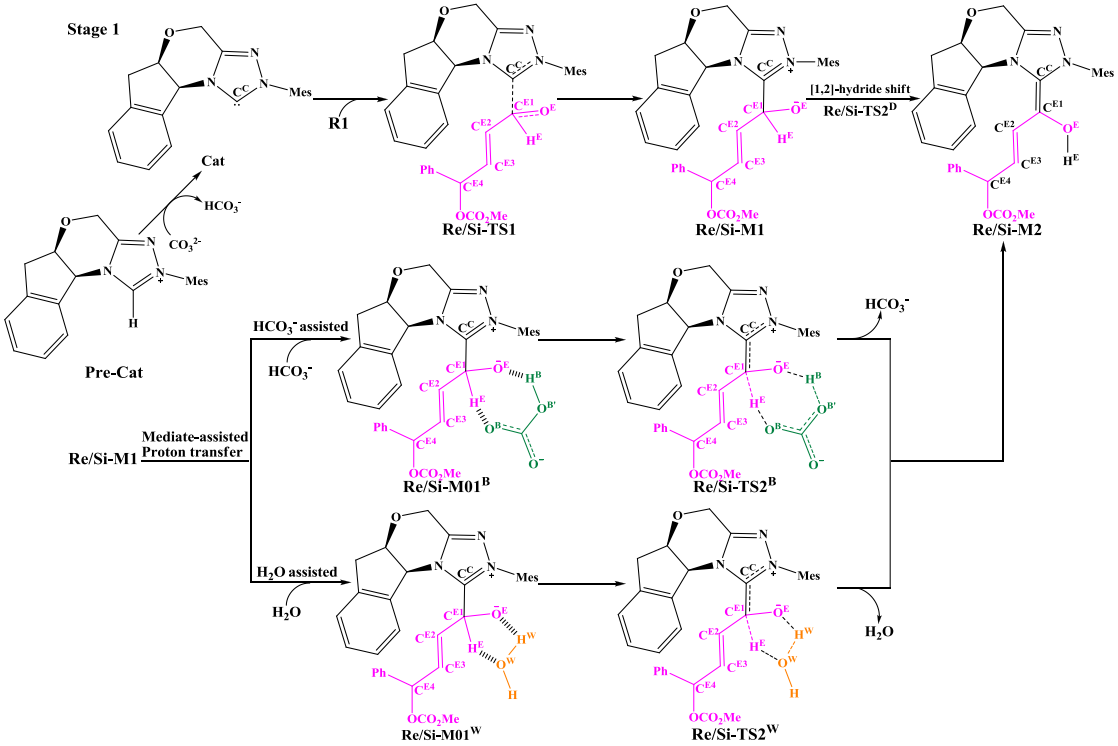

Scheme 3 The possible pathways of **Stage 1**

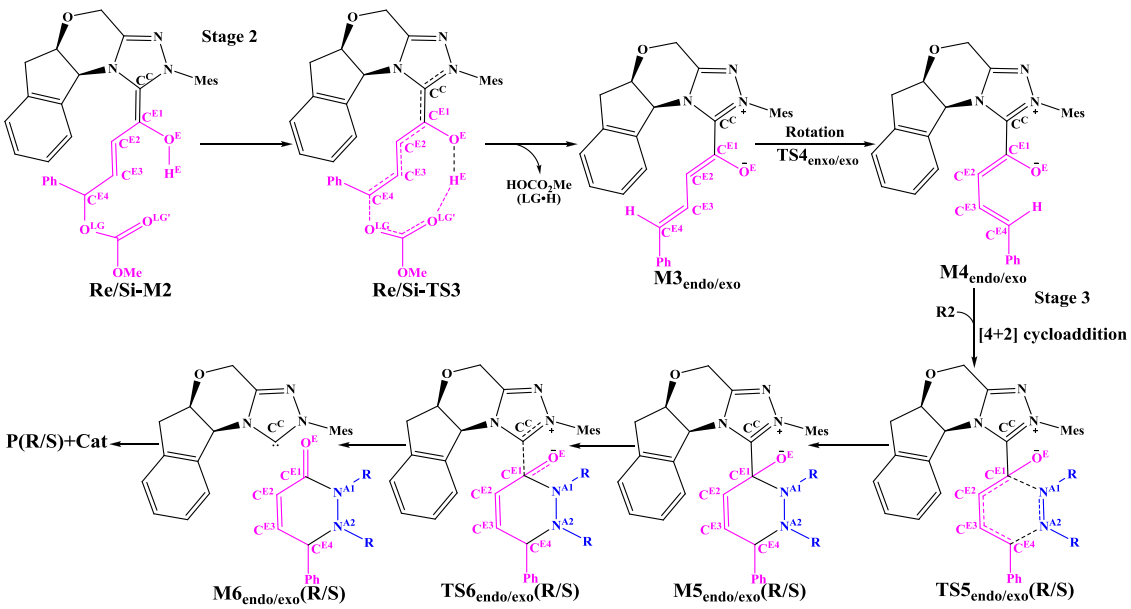

Scheme 4 The possible pathways of **Stages 2** and **3**

3.1 Stage 1: Formation of the Breslow intermediate

As shown in **Scheme 3**, it consists of two steps involved in **Stage 1**: (1) nucleophilic attack on the γ-oxidized enal **R1** by the catalyst **Cat**, (2) proton transfer of the formed intermediate to give the Breslow intermediate **Re/Si-M2**. **Fig. 1** and **Fig. 2** depict the Gibbs free energy profile and the optimized structures involved in **Stage 1**, respectively.

*3.1.1 Nucleophilic addition of **Cat** to **R1***. With the aid of CO_3^{2-} (derivative from the base K_2CO_3), deprotonation of the original catalyst **Pre-Cat** firstly occurs to yield the active catalyst **Cat** and HCO_3^- (conjugate acid of K_2CO_3, **Scheme 3**).[14a,18b] Then the coordinated zwitteronic intermediate **Re/Si-M1** is formed through the Re/Si-face nucleophilic attack on the C^{E1} atom of **R1** by the C^C atom in **Cat** via transition state **Re/Si-TS1**, respectively. The optimized geometries given in **Fig. 2** show that the distance of C^C–C^{E1} is shortened from 2.00/2.01 Å in transition state **Re/Si-TS1** to 1.56/1.55 Å in the intermediate **Re/Si-M1**, which implies the complexation of catalyst with reactant. The Gibbs free energy barrier of this addition step via **Re/Si-TS1** (12.41/9.71 kcal/mol, **Fig. 1**) reveals that the reaction can occur smoothly under the experimental condition.

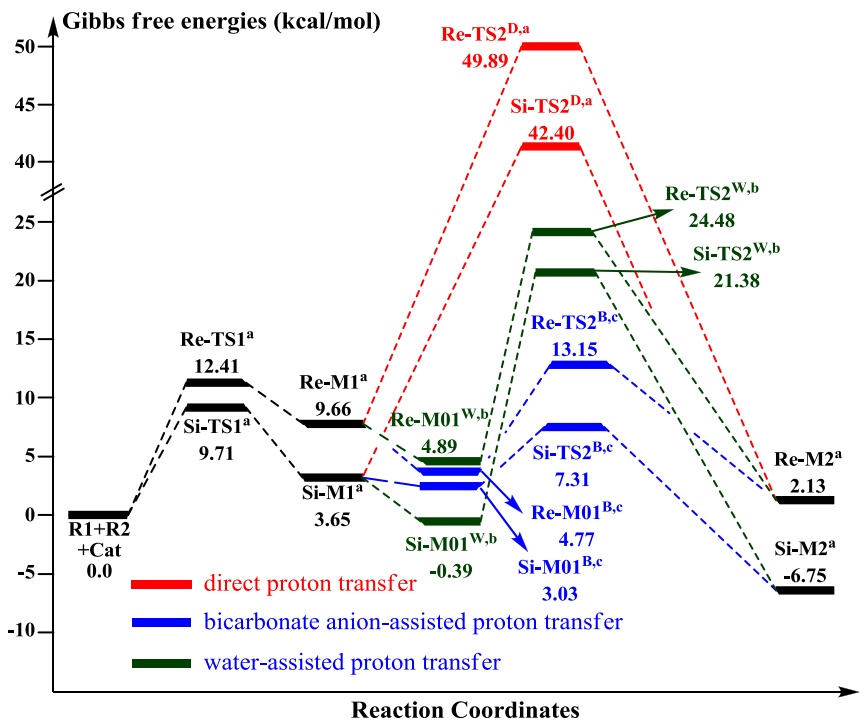

Fig. 1 The Gibbs free energy profiles of **Stage 1** ([a]adding the free energy of **R2**. [b]adding the free energies of H_2O and **R2**. [c]adding the free energies of bicarbonate anion and **R2**.)

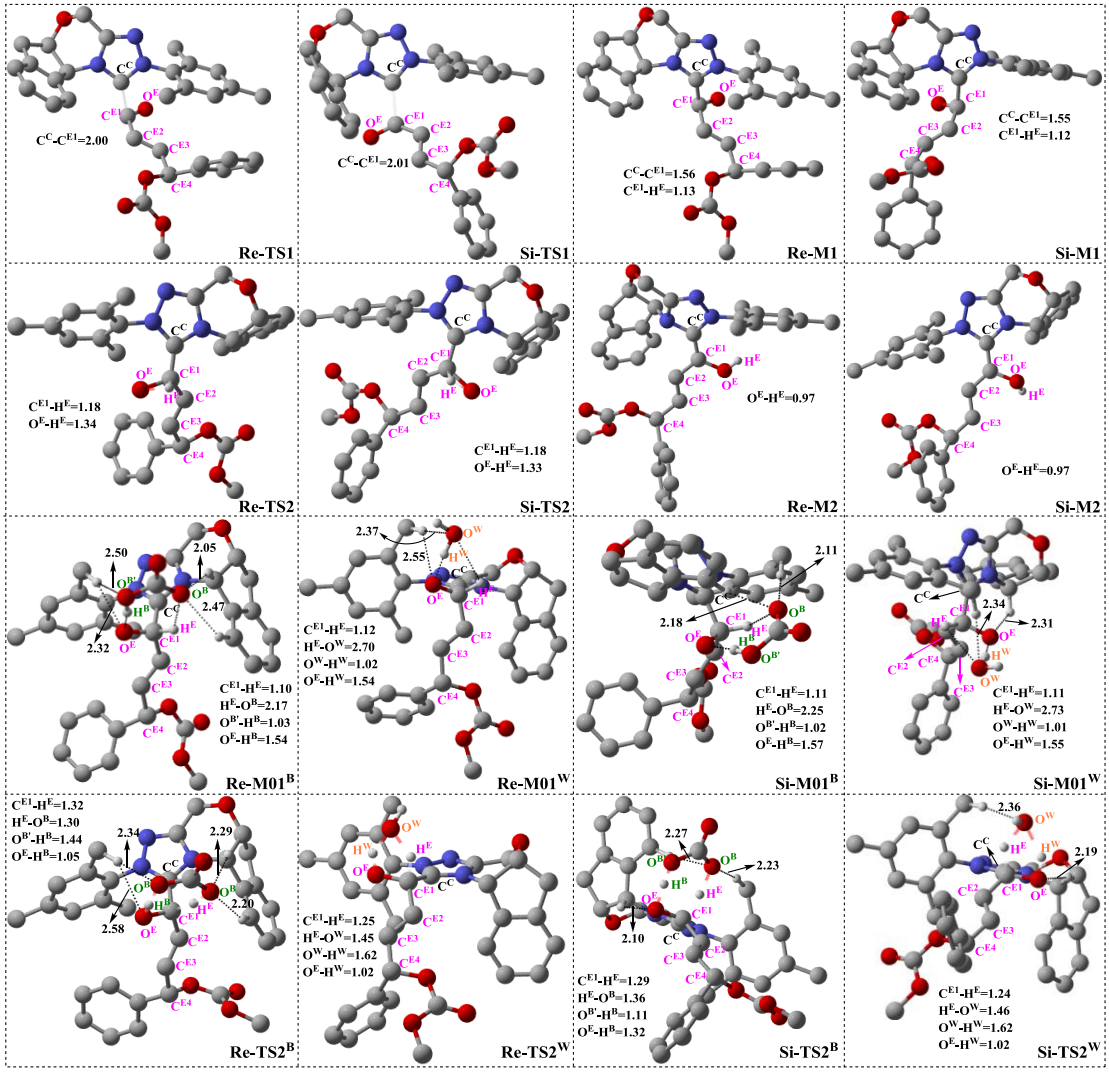

Fig. 2 The optimized structures and geometry parameters of the intermediates and transition states involved in **Stage 1** (distance in Å and most of the hydrogen atoms are omitted for sake of clarify)

3.1.2 1,2-proton transfer. The second step of **Stage 1** is the proton transfer process, by which the H^E transfers from C^{E1} to O^E atoms for the formation of Breslow intermediate. There are three possible pathways for the proton transfer process, in particular, the direct proton transfer process via the three-membered ring transition state **Re/Si-TS2^D**, the bicarbonate anion (HCO_3^-) assisted proton transfer process via the seven-membered ring transition state **Re/Si-TS2^B**, and the H_2O-assisted proton transfer process via the five-membered ring transition state **Re/Si-TS2^W**.

(i) Direct and HCO_3^--assisted proton transfer processes: The direct intramolecular proton transfer process via transition state **Re/Si-TS2^D** to form the stable Breslow intermediate **Re/Si-M2** with the free energy of 2.13/−6.75 kcal/mol,

encounters a significantly higher free energy barrier (49.89/42.40 kcal/mol, **Fig. 1**), indicating the direct proton transfer process is impossible to occur under the experimental conditions and such possibility is not likely in a non-polar aprotic medium such as THF. Notably, it has been reported that the generation of the Breslow intermediate could involve significant barriers unless a base/acid-assisted proton transfer mechanism is invoked. In view of this, the former formed HCO_3^--assisted proton transfer process, as opposed to a conventional pathway, has been taken into consideration. As illustrated in **Scheme 3**, the reaction precursor **Re/Si-M01^B** is formed by weak interaction between **Re/Si-M1** and HCO_3^-. Geometrical and structural parameters of the reaction precursor **Re/Si-M01^B** depicted in **Fig. 2** show that the intermolecular hydrogen bond makes the zwitterionic **Re/Si-M01^B** much stable. Then the proton H^E transfers from C^{E1} to O^B atoms, coupled with the proton H^B transferring to O^E atom via the seven-membered ring transition state **Re/Si-TS2^B**. The distances of C^{E1}–H^E, H^E–O^B, $O^{B'}$–H^B, and H^B–O^E in the transition state **Re/Si-TS2^B** are 1.32/1.29, 1.30/1.36, 1.44/1.11, and 1.05/1.32 Å, which reveals that the HCO_3^--assisted proton transfer step is a concerted but asynchronous process, the formation of the H^B–O^E bond (1.05/1.32 Å) is a little advanced than the formation of the H^E–O^B bond (1.30/1.36 Å) in transition state **Re/Si-TS2^B**. The distance between O^E and $H^{E(B)}$ atoms in the Breslow intermediate **Re/Si-M2** is 0.97/0.97 Å, demonstrating the full formation of the O^E–$H^{E(B)}$ bond. The energy barrier of this step is 13.15/7.31 kcal/mol (**Fig. 1**), which demonstrates that the HCO_3^--assisted proton transfer process occurs more easily than the direct proton transfer process under the experimental conditions. Moreover, we have tried, but failed to locate the HCO_3^--assisted five-membered (C^{E1}–H^E–O^B–H^B–O^E) ring transition state involved in the proton transfer process, which is easily re-optimized to the seven-membered one.

(ii) The H_2O-assisted proton transfer process: It is important at this juncture to infer that the catalytic reaction was carried out without N_2/Ar protection at room temperature. This phenomenon shows that there should be trace of water in the solvent, which will mediate the proton transfer and make the H_2O-assisted proton transfer pathway deemed feasible. Many other computational studies also demonstrated the similar important role of water or water cluster ($2H_2O$ cluster) in the catalytic reactions which involves the proton transfer without any protic mediator.[27] Prior to generating **Re/Si-M2**, **Re/Si-M1** and H_2O first form a complex (**Re/Si-M01^W**) through electrostatic attraction between the two components (the $2H_2O$ cluster

assisted proton transfer process have also been considered and discussed in ESI). The complex is enthalpically more stable (Enthalpy energies are provided in ESI), but less stable in free energy than **R1+R2+Cat**, which implies that the electrostatic attraction can contribute to pulling the two components together. After passing through a barrier of 24.48/21.38 kcal/mol (**Re/Si-TS2^{W}**), the Breslow intermediate **Re/Si-M2** is formed via a five-membered ring transition state (**Re/Si-TS2^{W}**). The gradually changed O^{E}–H^{W}, C^{E1}–H^{E}, and O^{W}–H^{E} distances for **Re/Si-M01^{W}** and **Re/Si-TS2^{W}** (**Fig. 2**) illustrate the proton transfer process.

Taken together, three possible pathways for the proton transfer process to afford **Re/Si-M2** have been suggested and studied. Based on the discussions above, one can conclude that the HCO_3^--assisted proton transfer for the formation of **Re/Si-M2** via the seven-membered ring transition state **Re/Si-TS2^{B}** (13.15/7.31 kcal/mol) is the most energetically feasible than others. In addition, we have failed to locate the transition state for the bimolecular proton transfer process between two **Re/Si-M1** molecules. This might be related to the high steric hindrance between the two structures, which makes it difficult by pulling the two molecules of **Re/Si-M1** together in a suitable orientation for the proton transfer.

3.2 Stage 2: Formation of the *cis*-dienolate **M4$_{endo/exo}$**

Scheme 4 presents the detailed mechanism of the remaining stages (**Stage**s **2** and **3**) of the catalytic reaction. There are also two steps involved in **Stage 2**: the removal of the leaving group (LG) and the rotation of C^{E2}–C^{E3} single bond. We term the *endo* when dienolate points on the same side of the indane, whereas dienolate pointed on the opposite side of the indane is named by *exo*.

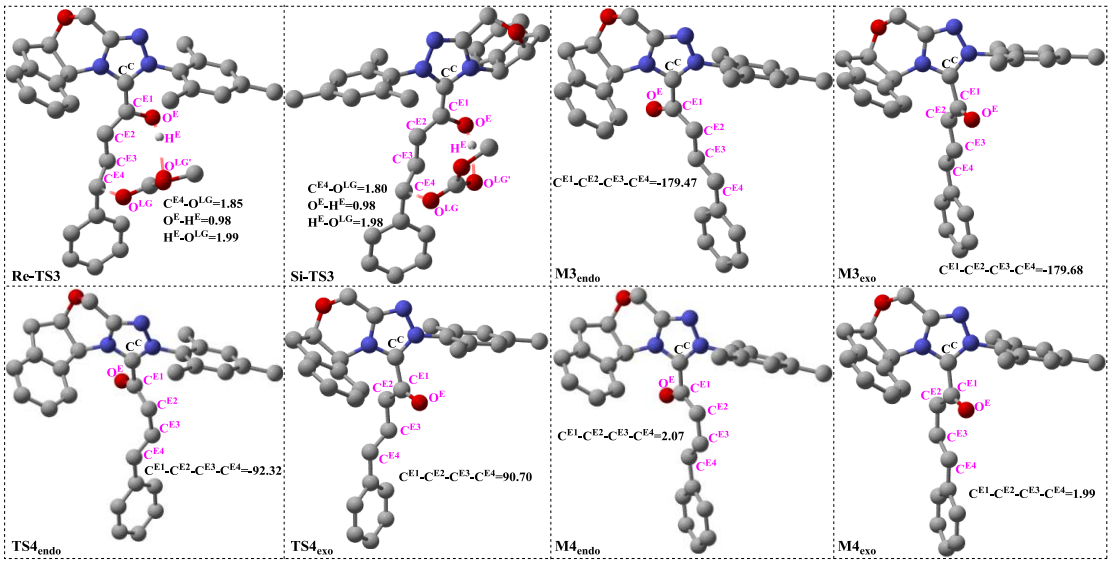

Fig. 3 The optimized structures and geometry parameters of the intermediates and transition states involved in **Stage 2** (distance in Å, dihedral in °, and most of the hydrogen atoms are omitted for sake of clarify)

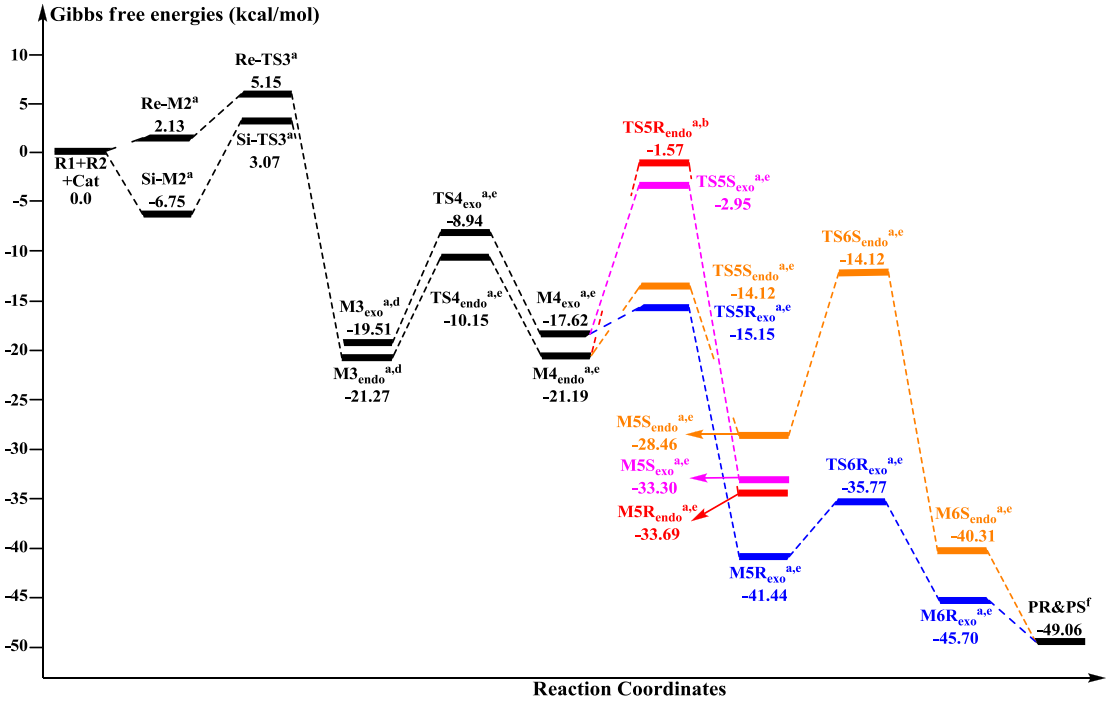

Fig. 4 The Gibbs free energy profiles of **Stage 2** and **Stage 3** ([a]adding the free energy of **R2**. [d]adding the free energy of **LGH** and **R2**. [e]adding the free energy of **LGH**. [f]adding the free energy of **Cat** and **LGH**.)

3.2.1 Removal of leaving group. In this step, the Breslow intermediate **Re/Si-M2** decomposes to the *trans*-dienolate **M3$_{endo/exo}$** by removal of the leaving group via

transition state **Re/Si-TS3**. The calculated results indicate that the breaking of C^{E4}–O^{LG} bond (1.85/1.80 Å, **Fig. 3**) is much more advanced at the **Re/Si-TS3** than the formation of the O^{LG}–H^{E} bond (1.99/1.98 Å, **Fig. 3**). The removal of leaving group in the **Re-M2** leads to the *trans*-dienolate $\mathbf{M3_{endo}}$, correspondingly, the **Si-M2** gives the *trans*-dienolate $\mathbf{M3_{exo}}$. The optimized structures depicted in **Fig. 3** show that the dienolate of $\mathbf{M3_{endo/exo}}$ is not stabilized by conjugation with the NHC but lies perpendicular to the N-heterocycle. Since the dienolate is blocked by the indane on one side and mesitylene on the other. The energy barrier for the removal of leaving group via transition state **Re/Si-TS3** is 5.15/3.07 kcal/mol (**Fig. 4**), which can proceed facilely under the experimental conditions.

3.2.2 Rotation of C^{E2}–C^{E3} bond. The next step in **Stage 2** is the rotation of C^{E2}–C^{E3} single bond to form the intermediate *cis*-dienolate $\mathbf{M4_{endo/exo}}$ via transition state $\mathbf{TS4_{endo/exo}}$. As depicted in **Scheme 2**, the reactant **R2** would addict to C^{E4} atom of *trans*-dienolate $\mathbf{M3_{endo/exo}}$ directly, however, it is difficult for the subsequent ring-closure process, which yields the *cis*-configured six-membered ring intermediate. Thus, the isomerization of the *trans*-dienolate to *cis*-dienolate would occur preferentially. The computations show that this rotation process occurs via $\mathbf{TS4_{endo/exo}}$ with an energy barrier of 11.12/10.57 kcal/mol (with respect to $\mathbf{M3_{endo/exo}}$), and brings the two C=C bonds (C^{E1}=C^{E2} and C^{E3}=C^{E4}) to the right relative conformation, which is necessary for the following [4 + 2] cycloaddition process with **R2**.

3.3 Stage 3: Formal [4 + 2] cycloaddition and regeneration of catalyst

The following process of the catalytic reaction is the [4 + 2] cycloaddition reaction. As shown in **Scheme 4**, **Stage 3** includes two process: (1) the formal [4 + 2] cycloaddition of *cis*-dienolate with **R2**, (2) dissociation of product with catalyst and regeneration of catalyst. The optimized structures involved in **Stage 3** are given in **Fig. 5**.

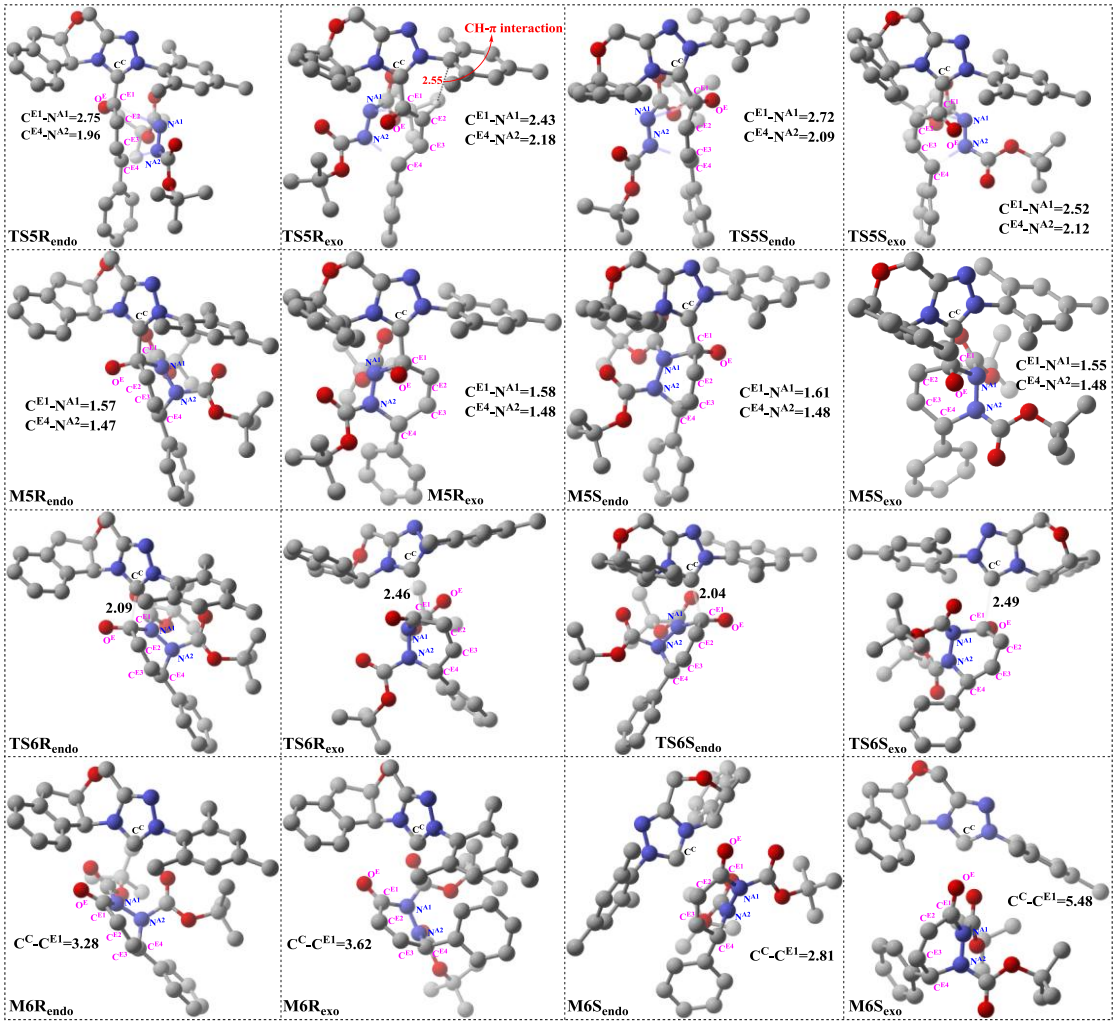

Fig. 5 The optimized structures and geometry parameters of the intermediates and transition states involved in **Stage 3** (distance in Å and most of the hydrogen atoms are omitted for sake of clarify)

3.3.1 Formal [4 + 2] cycloaddition. As mentioned above, the *cis*-dienolate intermediate **M4$_{endo/exo}$** is formed in the second step of **Stage 2** by the rotation of C^{E2}–C^{E3}, and the next step is the construction of the six-membered (C^{E1}–C^{E2}–C^{E3}–C^{E4}–N^{A2}–N^{A1}) heterocycle, which obviously needs to add the **R2**. By electrostatic attraction between C^{E1} and N^{A1} along with that between C^{E4} and N^{A2}, the six-membered ring is formed in **M5R/S$_{endo/exo}$** via transition state **TS5R/S$_{endo/exo}$** with approach of **M4$_{endo/exo}$** to **R2**. **Table 1** illustrates the possible reaction patterns for the formal [4 + 2] cycloaddition involved in **Stage 3**, there exists four possible reaction patterns for this step, because for either **M4$_{endo}$** or **M4$_{exo}$**, **R2** can attack from either their Re or Si face to participate in the reaction. As an important note, the chirality center assigned on C^{E4} atom is formed during the ring forming process, which

depends on the Re or Si face of **M4**$_{endo/exo}$ that **R2** gets close to.

Table 1 Possible reaction patterns for the [4 + 2] cycloaddition step in **Stage 3**

Configuration of **M4**	Addition face of **M4**	Chirality of C^{E4} atom
endo	Re	R
endo	Si	S
exo	Re	R
exo	Si	S

The geometrical parameters depicted in **Fig. 5** show that the formation of C^{E4}–N^{A2} bond is preferentially to the formation of C^{E1}–N^{A1} bond. This phenomenon indicates that the two bonds (i.e. C^{E1}–N^{A1} and C^{E4}–N^{A2}) are formed by a concerted but highly asynchronous manner. The free energy profile mapped in **Fig. 4** reveals that **M5R**$_{exo}$ is located 7.75/8.14/12.98 kcal/mol lower than **M5R**$_{endo}$/**M5S**$_{exo}$/**M5S**$_{endo}$ separately, which implies that **M5R**$_{exo}$ will be the significantly dominant isomer from the aspect of thermodynamics. In addition, the energy barriers of the cycloaddition step are 19.62 (**TS5R**$_{endo}$) and 7.07 (**TS5S**$_{endo}$) kcal/mol with respect to **M4**$_{endo}$ for *endo* addition, whereas these for *exo* addition are 2.47 (**TS5R**$_{exo}$) and 14.67 (**TS5S**$_{endo}$) kcal/mol with respect to **M4**$_{exo}$, respectively. Obviously, the *endo* addition for the formation of **M5R**$_{endo}$ and *exo* addition for the formation of **M5S**$_{exo}$ are unfavorable than the others, thus in the following parts, we think it is unnecessary to discuss these two possible reaction patterns. The formation of **M5R**$_{exo}$ costs the lowest energy barrier and the energy barrier of **TS5R**$_{exo}$ is 4.6 kcal/mol lower than that of **TS5S**$_{endo}$, which indicates that the formation of **M5R**$_{exo}$ is more energy favorable and supports the reported preference to form the R-configuration of the product.

3.3.2 Regeneration of the catalyst. Since in the first step of **Stage 3**, the six-membered cycloadduct is formed by [4 + 2] cycloaddition. The last process is the dissociation of catalyst with product, and this leads to the regeneration of the catalyst. As shown in **Fig. 3**, the distance between C^{C} atom and C^{E1} atom is increased from 2.46/2.04 Å in **TS6R**$_{exo}$/**TS6S**$_{endo}$ to 3.62/2.81 Å in **M6R**$_{exo}$/**M6S**$_{endo}$, and the free energy barrier of this step is 5.67/14.34 kcal/mol, revealing that the dissociation process is a facilitated process and the catalyst is easy to regenerate.

3.3 Origin of the enantioselectivity

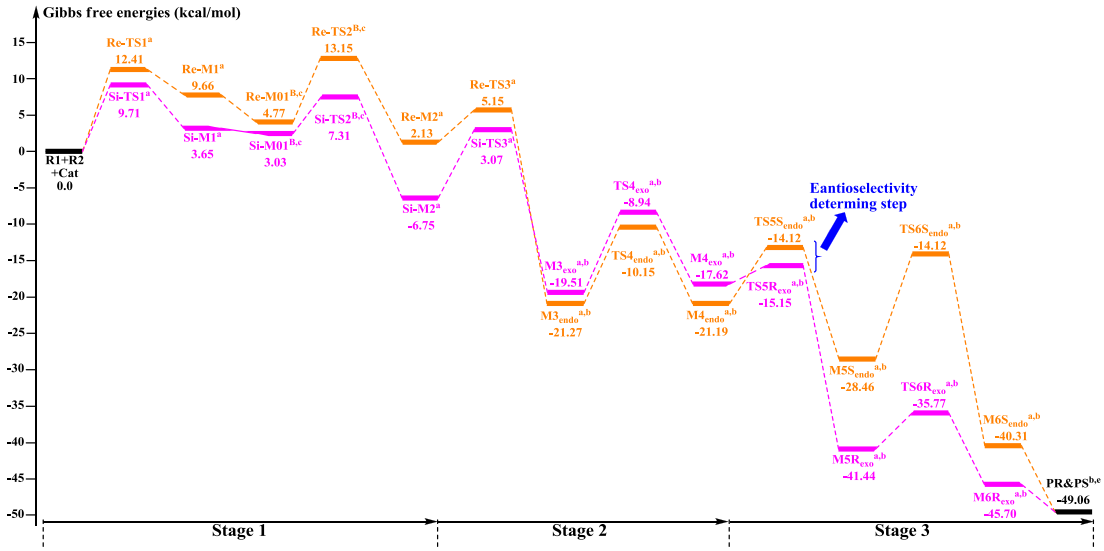

Fig. 6 The entire energy profiles of the NHC-catalyzed [4 + 2] annulation reaction

In **Fig. 6**, only the most energy favorable pathways involved in the three states are shown. As discussed above, **Stages 1** and **3** both contain more than one step, thus we only provided the energy profiles of pathways with the lowest energy barriers in **Fig. 6**. For **Stage 1**, the HCO_3^--assisted proton transfer mechanism is the most favorable pathways associated with the energy barrier of 13.15/7.31 kcal/mol (**Re/Si-TS2^B**). In **Stage 3**, the *exo* addition of **R2** to **M4R$_{exo}$** and *endo* addition of **R2** to **M4S$_{endo}$** are energy favorable. Moreover, as can be seen in **Fig. 6**, the reaction pathway associated with the formation of product **PR** is the main reaction pathway, and the rate-determining step of the main reaction pathway is identified to be the C–C single bond rotation step with the free energy of 10.57 kcal/mol (**TS4$_{exo}$**). Furthermore, the chirality center (C^{E4} atom) is emerged in the formal [4 + 2] cycloaddition step of **Stage 3**, so we think this step is the enantioselectivity determining step (R-configuration is predominant).

To explore the reason of the enantioselectivity, we performed the distortion-interaction analysis.[28] The relative energies of the transition state **TS5R$_{exo}$** and **TS5S$_{endo}$** parallel the stabilities of the corresponding product-NHC complexes (**M5R$_{exo}$** vs. **M5S$_{endo}$**). As both transition states are significantly affected by charge delocalization and steric configuration, we first employed the diastereomeric product complexes **M5R$_{exo}$** and **M5S$_{endo}$** to elucidate the origin of the selectivity. For both structures, we analyzed the contributions of distortion, assuming that the difference in transition state energies will be of similar origin. Here the activation energy is divided

into two components, the distortion energy (E_{dist}) and interaction energy (E_{int}).[28] The distortion energy involves geometric and electronic changes to deform the reactants into their transition state geometry, which contains bond stretching, angle decrease or increase, dihedral change, and so on. The interaction energy includes exchange-repulsive and stabilizing electrostatic, polarization, and orbital effects in the transition state structure.

From the results in **Table 2**, one can conclude that the **M4R$_{exo}$** in **M5R$_{exo}$** is slightly more distorted [$\Delta\Delta E_{dist}$(**M4$_{exo}$**)] from its equilibrium geometry (**M4R$_{exo}$**) than **M4S$_{endo}$** in **M5R$_{endo}$**. This is largely counterbalanced by the distortion of the **R2** [$\Delta\Delta E_{dist}$(**R2**)], which is more distorted in **M5S$_{endo}$**. And the larger distortion of the **R2** in **M5S$_{endo}$** should be the main reason that the free energy of **M5R$_{endo}$** is much lower than that of **M5S$_{endo}$**.

Table 2 Contributions of distortion (dist) to the stabilities of the key transition states (**TS5R$_{exo}$** and **TS5S$_{endo}$**) and the product complexes (**M5R$_{exo}$** and **M5S$_{endo}$**) [in kcal/mol; M06-2X/6-31G(d, p)/IEF-PCM$_{THF}$]

	$\Delta\Delta G$	$\Delta\Delta E_{dist}$(M4$_{endo/exo}$)	$\Delta\Delta E_{dist}$(R2)
M5S$_{endo}$	+12.98	0.0	+27.54
M5R$_{exo}$	0.0	+4.96	0.0
TS5S$_{endo}$	+1.03	+5.76	0.0
TS5R$_{exo}$	0.0	0.0	+1.47

The analysis of the stereocontrolling TSs is also carried out to figure out the factors that controlling the stereoselectivity. The distortion results demonstrate that the **M4S$_{endo}$** in **TS5S$_{endo}$** is more distorted than **M4R$_{exo}$** in **TS5$_{exo}$**, whereas the **R2** is slightly more distorted in **TS5R$_{exo}$** than that in **TS5S$_{endo}$**. As could be anticipated, the **M4R$_{exo}$** benefits from the lower **ΔE_{dist}** value and the distortion of **R2** is offset by large **ΔE_{dist}** penalties of **M4S$_{endo}$**. Moreover, the transition state with C^{E1} of the dienolate pointing toward the mesitylene (**TS5R$_{exo}$**) is lower in energy than when it is toward the indane due to a CH-π interaction between CH of the dienolate and the aromatic ring. Specifically, the inner hydrogen on the dienolate carbon is just 2.55 Å from C^{E1} to mesitylene (**Fig. 5**) and the distance between C-H of the dienolate and the center of the aromatic ring is ~2.90 Å, well within the combined van der Waals distance of 2.90 Å. For such CH-π interactions have been observed in the transition states of Diels-Alder reactions, sulfide oxidations, and hydride reductions.[29] On the whole, the less distortion and the existence of CH-π interaction make the lower energy barrier of

TS5R$_{exo}$ and the formation of the R-configuration isomer preferred kinetically.

The computed energy difference between the diastereomeric **TS5$_{exo}$** and **TS5$_{endo}$** is 4.6 kcal/mol, which corresponds to an enantiomeric excess of >99% in favor of the R isomer. This prediction is in good accordance with the experimentally observed *ee* of 99%.

4. Conclusion

In this present study, we have analyzed the [4 + 2] annulation reaction between γ-oxidized enals (**R1**) and di-*tert*-butyl azodicatboxylate (**R2**) catalyzed by N-heterocyclic carbene (NHC) using density functional theory. On the basis of our calculations, the reaction is demonstrated to occur through three elementary stages, and for each stage, more than on possible pathway that involved different participation molecules has been investigated. The calculated results reveal that the most favorable pathway contains six elementary steps: the NHC catalyst first reacts with **R1** to initiate the reaction, and then the Breslow intermediate is formed by HCO_3^--assisted proton process. Subsequently, the removal of leaving group concerted with abstracting the hydrogen from O^E atom and next step is the isomerization process to give the *cis*-dienolate. The fifth step is the *endo*/*exo* [4 + 2] addition reaction of **R2** to *cis*-dienolate and in the final step, the NHC catalyst is regenerated and the [4 + 2] cycloaddition products **PR**&**PS** are released. The enantioselectivity associated with the chiral carbon center (C^{E4} atom) turns out to be determined by the Re or Si face addition of **R2** with **M4$_{endo/exo}$**. All the calculations are in consistent with the experimental results.

Moreover, the distortion scale of **M5** (**M5R$_{exo}$** and **M5S$_{endo}$**) and **TS5** (**TS5R$_{exo}$** and **TS5S$_{endo}$**) as well as the CH-π interaction are the key factors that control the stereoselectivity. The use of the bicarbonate anion as the protic medium to assist the proton transfer will provide a new clue for this kind of reaction without any other protic additive.

Acknowledgements

The work described in this paper was supported by the National Natural Science Foundation of China (No. 21303167), China Postdoctoral Science Foundation (No. 2013M530340) and Excellent Doctoral Dissertation Engagement Fund of Zhengzhou University in 2014.

References

1. (a) F. Glprious, *Springer-Verlag: Berlin, Heidelberg*, 2006, **21**, 1; (b) S. P. Nolan, *Acc. Chem. Res.*, 2010, **44**, 91; (c) D. Zhang and G. F. Zi, *Chem. Soc. Rev.*, 2015, **44**, 1898; (d) C. Chen, M. H. Kim and S. H. Hong, *Org. Chem. Front.*, 2015, **2**, 241.

2. (a) D. Enders, O. Niemeier and A. Henseler, *Chem. Rev.*, 2007, **107**, 5606; (b) F. Glorius and K. Hirano, *Springer-Verlag: Berlin, Heidelberg*, 2008, **2**, 159; (c) J. L. Moore and T. Rovis, *Top. Curr. Chem.*, 2010, **291**, 77; (d) D. Enders and T. Balensiefer, *Acc. Chem. Res.*, 2004, **37**, 534; (e) V. Nair, S. Vellalath and B. P. Babu, *Chem. Soc. Rev.*, 2008, **37**, 2691; (f) M. Fèvre, J. Pinaud, Y. Gnanou, J. Vignolle and D. Taton, *Chem. Soc. Rev.*, 2013, **42**, 2142.

3. (a) J. Kaeobamrung, M. C. Kozlowski and J. W. Bode, *Proc. Natl. Acad. Sci. U. S. A.*, 2010, **107**, 20661; (b) S. J. Ryan, L. Candish and D. W. Lupton, *J. Am. Chem. Soc.*, 2011, **133**, 4694; (c) T. Y. Jian, L. He, C. Tang and S. Ye, *Angew. Chem. Int. Ed.*, 2011, **50**, 9104; (d) E. M. Phillips, M. Wadamoto, A. Chan and K. A. Scheidt, *Angew. Chem. Int. Ed.*, 2007, **46**, 3107; (e) D. Enders, A. Grossmann, J. Fronert and G. Raabe, *Chem. Commun.*, 2010, **46**, 6282; (f) T. Ema, Y. Oue, K. Akihara, Y. Miyazaki and T. Sakai, *Org. Lett.*, 2009, **11**, 4866; (g) D. A. DiRocco and T. Rovis, *J. Am. Chem. Soc.*, 2011, **133**, 1040; (h) T. Jousseaume, N. E. Wurz and F. Glorious, *Angew. Chem. Int. Ed.*, 2011, **50**, 1410; (i) Q. Kang and Y. Zhang, *Org. Biomol. Chem.*, 2011, **9**, 6715; (j) A. Lee and K. A. Scheidt, *Chem. Commun.*, 2015, **51**, 3407; (k) H. Lu, J. Y. Liu, C. G. Li, J. B. Lin, Y. M. Liang and P. F. Xu, *Chem. Commun.*, 2015, **51**, 4473; (l) X. K. Chen, X. Q. Fang and Y. R. Chi, *Chem. Sci.*, 2013, **4**, 2613.

4. (a) X. N. Wang, P. L. Shao, H. Lv and S. Ye, *Org. Lett.*, 2009, **11**, 4029; (b) X. L. Huang, X. Y. Chen and S. Ye, *J. Org. Chem.*, 2009, **74**, 7585; (c) J. Douglas, J. E. Taylor, G. Churchill, A. M. X. Slawin and A. D. Smith, *J. Org. Chem.*, 2013, **78**, 3925; (d) X. N. Wang, L. T. Shen and S. Ye, *Org. Lett.*, 2011, **13**, 6382; (e) T. Wang, X. L. Huang and S. Ye, *Org. Biomol. Chem.*, 2010, **8**, 5007; (f) H. M. Zhang, Z. H. Gao and S. Ye, *Org. Lett.*, 2014, **16**, 3079.

5. X. N. Wang, L. T. Shen and S. Ye, *Chem. Commun.*, 2011, **47**, 8388.

6. (a) S. M. Leckie, B. Brown, D. Pryde, T. Lebl, A. M. Z. Slawin and A. D. Smith, *Org. Biomol. Chem.*, 2013, **11**, 3230; (b) T. Y. Jian, X. Y. Chen, L. H. Sun and S. Ye, *Org. Biomol. Chem.*, 2013, **11**, 158; (c) T. Y. Jian, P. L. Shao and S. Ye, *Chem. Commun.*, 2011, **47**, 2381.

7. (a) C. Burstein and F. Glorius, *Angew. Chem. Int. Ed.*, 2004, **43**, 6205; (b) S. S. Sohn, E. L. Rosen and J. W. Bode, *J. Am. Chem. Soc.*, 2004, **126**, 14370; (c) V. Nair, S. Vellalath, M. Poonoth and E. Suresh, *J. Am. Chem. Soc.*, 2006, **128**, 8736; (d) D. E. A. Raup, B. Cardinal-David, D. Holte and K. A. Scheidt, *Nat. Chem.*, 2010, **2**, 766; (e) X. D. Zhao, D. A. DiRocco and T. Rovis, *J. Am. Chem. Soc.*, 2011, **133**, 12466; (f) H. Lv, W. Q. Jia, L. H. Sun and S. Ye, *Angew. Chem. Int. Ed.*, 2013, **52**, 8607.

8. (a) M. He, J. R. Struble and J. W. Bode, *J. Am. Chem. Soc.*, 2006, **128**, 8418; (b) C. Burstein, S. Tschan, X. L. Xie and F. Glorius, *Synthesis*, 2006, 2418; (c) M. Wadamoto, E. M. Phillips, T. E. Reynolds and K. A. Scheidt, *J. Am. Chem. Soc.*, 2007, **129**, 10098; (d) V. Nair, R. R. Paul, K. C. S. Lakshmi, R. S. Menon, A. Jose and C. R. Sinu, *Tetrahedron Lett.*, 2011, **52**, 5992; (e) X. Q. Fang, X. K. Chen and Y. R. Chi, *Org. Lett.*, 2011, **13**, 4708.

9. (a) D. A. DiRocco and T. Rovis, *J. Am. Chem. Soc.*, 2011, **133**, 10402; (b) X. Fang, X. Chen, H. Lv and Y. R. Chi, *Angew. Chem. Int. Ed.*, 2011, **50**, 11782; (c) L. H. Sun, Z. Q. Liang, W. Q. Jia and S. Ye, *Angew. Chem. Int. Ed.*, 2013, **52**, 5803.

10. L. M. Fang, F. Wang, P. J. Chua, Y. B. Lv, L. J. Zhong and G. F. Zhong, *Org. Lett.*, 2012, **14**, 2894.

11. (a) S. H. Hu, B. Y. Wang, Y. Zhang, W. F. Tang, M. Y. Fang, T. Lu and D. Du, *Org. Biomol. Chem.*, 2015, DOI: 10.1039/C5OB00176E; (b) S. R. Yetra, S. Mondal, E. Suresh and A. T. Biju, *Org. Lett.*,

2015, **17**, 1417; (c) J. D. Tessier, E. A. O'Bryan, T. B. H. Schroeder, D. T. Cohen and K. A. Scheidt, *Angew. Chem. Int. Ed.*, 2012, **124**, 5047; (d) Z. Q. Liang, Z. H. Guo, W. Q. Jia and S. Ye, *Chem. A Eur. J.*, 2015, **21**, 1868; (e) C. Guo, M. Schedler, C. G. Daniliuc and F. Glorius, *Angew. Chem. Int. Ed.*, 2014, **53**, 10232; (f) A. G. Kravina, J. Mahatthananchai and J. W. Bode, *Angew. Chem. Int. Ed.*, 2012, **51**, 9433; (g) Y. Zhang, Y. Y. Lu, W. F. Tang, T. Lu and D. Du, *Org. Biomol. Chem.*, 2014, **12**, 3009.

12. (a) J. Izquierdo, A. Orue and K. A. Scheidt, *J. Am. Chem. Soc.*, 2013, **135**, 10634; (b) Y. W. Xie, Y. L. Que, T. J. Li, L. Zhu, C. X. Yu and C. S. Yao, *Org. Biomol. Chem.*, 2015, **13**, 1829; (c) H. Lv, W. Q. Jia, L. H. Sun and S. Ye, *Angew. Chem. Int. Ed.*, 2013, **125**, 8769.

13. (a) J. M. Mo, X. K. Chen and Y. R. Chi, *J. Am. Chem. Soc.*, 2012, **134**, 8810; (b) X. Y. Chen, F. Xia, J. T. Cheng and S. Ye, *Angew. Chem. Int. Ed.*, 2013, **52**, 10644; (c) R. Liu, C. X. Yu, Z. X. Xiao, T. J. Li, X. S. Wang, Y. W. Xie and C. S. Yao, *Org. Biomol. Chem.*, 2014, **12**, 1885; (d) M. Wang, Z. J. Huang, J. F. Xu and Y. R. Chi, *J. Am. Chem. Soc.*, 2014, **136**, 1214.

14. (a) J. Mahatthananchai and J. W. Bode, *Acc. Chem. Res.*, 2013, **47**, 696; (b) R. C. Johnston, D. T. Cohen, C. C. Eichman, K. A. Scheidt and P. H. Y. Cheong, *Chem. Sci.*, 2014, **5**, 1974; (c) S. E. Allen, J. Mahatthananachai, J. W. Bode and M. C. Kozlowski, *J. Am. Chem. Soc.*, 2012, **134**, 12098; (d) P. Verma, P. A. Patni and R. B. Sunoj, *J. Org. Chem.*, 2011, **76**, 5606; (e) Z. Y. Li, D. H. Wei, Y. Wang, Y. Y. Zhu and M. S. Tang, *J. Org. Chem.*, 2014, **79**, 3069.

15. (a) D. H. Wei, Y. Y. Zhu, C. Zhang, D. Z. Sun, W. J. Zhang and M. S. Tang, *J. Mol. Catal. A: Chem.*, 2011, **334**, 108;(b) M. M. Zhang, D. H. Wei, Y. Wang, S. J. Li, J. F. Liu, Y. Y. Zhu and M. S. Tang, *Org. Biomol. Chem.*, 2014, **12**, 6374.

16. W. J. Zhang, Y. Y. Zhu, D. H. Wei, Y. X. Li and M. S. Tang, *J. Org. Chem.*, 2012, **77**, 10729.

17. W. J. Zhang, D. H. Wei and M. S. Tang, *J. Org. Chem.*, 2013, **78**, 11849.

18. (a) T. Liu, S. M. Han, L. L. Han, L. Wang, X. Y. Cui, C. Y. Du and S. W. Bi, *Org. Biomol. Chem.*, 2015, **13**, 3654; (b) Q. Zhang, H. Z. Yu and Y. Fu, *Org. Chem. Front.*, 2014, **1**, 614; (c) Y. Qiao and K. L. Han, *Org. Biomol. Chem.*, 2012, **10**, 7689; (d) Y. Wang, D. H. Wei, Z. Y. Li, Y. Y. Zhu and M. S. Tang, *J. Phys. Chem. A*, 2014, **118**, 4288; (e) F. Godin, M. Duplessis, C. Buonomano, T. Trinh, K. Houde, D. Chapdelaine, J. Rodrigue, A. B. Outros and Y. Guindon, *Org. Chem. Front.*, 2014, **1**, 974; (f) Y. M. Chen, G. A. Chass and D. C. Fang, *Phys. Chem. Chem. Phys.*, 2014, **16**, 1078; (g) Y. Li and D. C. Fang, *Phys. Chem. Chem. Phys.*, 2014, **16**, 15224; (h) Y. Wang, D. H. Wei, W. J. Zhang, Y. Y. Wang, Y. Y. Zhu, Y. Jia and M. S. Tang, *Org. Biomol. Chem.*, 2014, **12**, 7503.

19. (a) Y. Qiao, K. L. Han and C. G. Zhan, *Org. Biomol. Chem.*, 2014, **12**, 2214; (b) D. H. Wei, B. L. Lei, M. S. Tang and C. G. Zhan, *J. Am. Chem. Soc.*, 2012, **134**, 10436; (c) D. M. Li, Y. Wang and K. L. Han, *Coord. Chem. Rev.*, 2012, **256**, 1137; (d) D. M. Li, X. Q. Huang and K. L. Han, *J. Am. Chem. Soc.*, 2011, **133**, 7416.

20. (a) Y. Ooyama, K. Uenaka and J. Ohshita, *Org. Chem. Front.*, 2015, DOI: 10.1039/C5QO00050E; (b) Y. Li and Z. Y. Lin, *Org. Chem. Front.*, 2014, **1**, 1188;(c) A. N. Hancock, Y. Kavanagh and C. H. Schiesser, *Org. Chem. Front.*, 2014, **1**, 645; (d) D. Leboeuf, M. Gaydou, Y. H. Wang and A. M. Echavarren, *Org. Chem. Front.*, 2014, **1**, 759; (e) M. Quan, G. Q. Yang, F. Xie, L. Gridney and W. Zhang, *Org. Chem. Front.*, 2015, **2**, 398; (f) L. Zhang and D. C. Fang, *J. Org. Chem.*, 2013, **78**, 2405; (g) J. Y. Tao, D. C. Fang and G. A. Chass, *Phys. Chem. Chem. Phys.*, 2012, **14**, 6937.

21. M. J. Frisch, G. W. Trucks, H. B. Schlegel, G. E. Scuseria, M. A. Robb, J. R. Cheeseman, G. Scalmani, V. Barone, B. Mennucci, G. A. Petersson, H. Nakatsuji, M. Caricato, X. Li, H. P. Hratchian, A. F. Izmaylov, J. Bloino, G. Zheng, J. L. Sonnenberg, M. Hada, M. Ehara, K. Toyota, R. Fukuda,, M. I. J. Hasegawa, T. Nakajima, Y. Honda, O. Kitao, H. Nakai, T. Vreven, J. A. Montgomery Jr., J. E. Peralta,

F. Ogliaro, M. Bearpark, J. J. Heyd, E. Brothers, K. N. Kudin, V. N. Staroverov, R. Kobayashi, J. Normand, K. Raghavachari, A. Rendell, J. C. Burant, S. S. Iyengar, J. Tomasi, M. Cossi, N. Rega, J. M. Millam, M. Klene, J. E. Knox, J. B. Cross, V. Bakken, C. Adamo, J. Jaramillo, R. Gomperts, R. E. Stratmann, O. Yazyev, A. J. Austin, R. Cammi, C. Pomelli, J. W. Ochterski, R. L. Martin, K. Morokuma, V. G. Zakrzewski, G. A. Voth, P. Salvador, J. J. Dannenberg, S. Dapprich, A. D. Daniels, Ö. Farkas, J. B. Foresman, J. V. Ortiz, J. Cioslowski and D. J. Fox, *GAUSSIAN 09* (*Revision C.01*), Gaussian, Inc., Wallingford, CT, 2010.

22. (a) Y. Zhao and D. G. Truhlar, *Theor. Chem. Acc.*, 2008, **120**, 215; (b) Y. Zhao and D. G. Truhlar, *Acc. Chem. Res.*, 2008, **41**, 157; (c) W. J. Zhang, D. G. Truhlar and M. S. Tang, *J. Chem. Theory Comput.*, 2013, **9**, 3965.

23. (a) B. Mennucci and J. Tomasi, *J. Chem. Phys.*, 1997, **106**, 5151; (b) V. Barone and M. Cossi, *J. Phys. Chem. A*, 1998, **102**, 1995.

24. (a) C. Gonzalez and H. B. Schlegel, *J. Chem. Phys.*, 1989, **90**, 2154; (b) C. Gonzalez and H. B. Schlegel, *J. Phys. Chem.*, 1990, **94**, 5523.

25. (a) A. E. Reed and F. Weinhold, *J. Chem. Phys.*, 1983, **78**, 4066;(b) J. P. Foster and F. Weinhold, *J. Am. Chem. Soc.*, 1980, **102**, 7211; (c) E. D. Glendening, A. E. Reed, J. E. Carpenter and F. Weinhold, *NBO Version 3.1*.

26. C. Y. Legault, *CYLview, 1.0b; Université de Sherbrooke, 2009 (http://www.cylview.org)*.

27. (a) L. L. Zhao, M. W. Wen and Z. X. Wang, *Eur. J. Org. Chem.*, 2012, 3531; (b) E. Mercier, B. Fonovic, C. Henry, O. Kwon and T. Dudding, *Tetrahedron Lett.*, 2007, **48**, 3617; (c) Y. Liang, S. Liu, Y. Z. Xia, Y. H. Li and Z. X. Yu, *Chem. Eur. J.*, 2008, **14**, 4361; (d) Y. Xia, Y. Liang, Y. Chen, M. Wang, L. Jiao, F. Huang, S. Liu, Y. Li and Z. X. Yu, *J. Am. Chem. Soc.*, 2007, **129**, 3470; (e) Y. Liang, S. Liu and Z. X. Yu, *Synlett.*, 2009, 905; (f) Y. Z. Xia, A. S. Dudnik, Y. H. Li and V. Gevorgyan, *Org. Lett.*, 2010, **12**, 5538; (g) Y. Z. Xia and G. P. Huang, *J. Org. Chem.*, 2010, **75**, 7842; (h) A. S. Dudnik, Y. Z. Xia, Y. H. Li and V. Gevorgyan, *J. Am. Chem. Soc.*, 2010, **132**, 7645.

28. C. Y. Legault, Y. Garcia, C. A. Merlic and K. N. Houk, *J. Am. Chem. Soc.*, 2007, **129**, 12664.

29. (a) R. Gordillo and K. N. Houk, *J. Am. Chem. Soc.*, 2006, **128**, 3543; (b) C. D. Anderson, T. Dudding, R. Gordillo and K. N. Houk, *Org. Lett.*, 2008, **10**, 2749; (c) M. A. M. Capozzi, C. Centrone, G. Fracchiolla, F. Naso and C. Cardellicchio, *Eur. J. Org. Chem.*, 2011, 4327; (d) O. Gutierrez, R. G. Iafe and K. N. Houk, *Org. Lett.*, 2009, **11**, 4298.